

The Application of Photoelectric Effect in Superconducting Materials

Tianchen Guo

Shanghai Pudong Dongding Foreign Language School, No.2151 Gong ji Rd, Huinan town, Pudong District, Shanghai, PRC 200135

mitchellguo2005@163.com

Abstract. In this paper, the history of superconducting materials and the superconducting phenomena are first briefly described, followed by a corresponding introduction to the characterization techniques that may be used in the study of superconducting materials. For example, scanning tunneling microscope is used to demonstrate the hole Fermi and electron Fermi surfaces in Fe-based superconducting materials. Fourier-transform infrared (FTIR) spectroscopy is used to study the symmetry of the superconducting band gap in Fe-based superconducting materials. Four-probe electrical transport measurements are used to measure the resistivity of superconducting materials. Angle-resolved photoemission spectroscopy (ARPES) is used to study the multi-orbital-to-electron structure of Fe-based superconducting materials, the symmetry of the superconducting band gap and its size, the various ordered states to electron. The use of ARPES to study the multi-orbital pair electron structure of Fe-based superconducting materials, the symmetry and size of the superconducting energy band gap, the structure of the various ordered states and the possible electronic coupling modes, etc. have made a great contribution to the exploration and study of superconducting materials.

Keywords: superconducting phenomena, scanning tunneling microscope, Fourier-transform infrared spectroscopy, four-probe electrical transport measurements, photoelectric effect, angle resolved photoemission spectroscopy.

1. Introduction

A superconducting material is one that exhibits superconducting properties under certain conditions [1], mainly characterized by its complete antimagnetism and zero resistance. The industrial use of superconducting materials is mainly used in important fields such as information and energy, transportation and power systems, scientific instruments and equipment, medical fields, and military equipment, which effectively advance the economy and civilization of the present society. At present, the main research directions of superconducting materials are iron-based superconducting materials, hydrogen-rich superconducting materials and copper-based superconducting materials. In addition to the current attention and research on room temperature superconducting materials in the scientific community, the structural and performance characterization of these materials is also a very important research direction. For this reason, this paper introduces the history of the development of superconducting materials and related mechanisms, and highlights the important role of material characterization and photoelectric effect in the optimization of superconducting material performance.

2. The development history of the superconducting phenomena

In 1911, the famous physicist Heike Kamerlingh Onnes discovered that mercury had zero resistance at temperatures below 4.2K. With further research, he discovered that many elements and various alloys possessed a similar zero resistance to that of mercury at low temperatures, and due to the specificity of this zero resistance phenomenon, Heike Kamerlingh Onnes called this phenomenon superconductivity [2]. In 1933, Walther Meissner and Robert Ochsenfeld discovered that a characteristic feature of superconductors is that when a superconducting material enters the superconducting state, all the internal magnetic flux of the material is emitted to the outside of the material, which results in the magnetic induction value inside the material remaining zero, and this phenomenon was later defined as the Meissner Effect [3]. The two scientists Cornelis Gorter and Hendrik Casimir proposed the two-fluid model in 1934, followed by two scientists named Fritz London and Heinz London in the following year who further developed the two-fluid model of Cornelis Gorter and Hendrik Casimir by incorporating electromagnetic theory[4]. In 1950, the London equation was modified by physicist Pippard, which called pippard [nonlocal] theory [5]. In the same year, the Soviet scientists Vitaly Ginzburg and Lev Davidovich Landau proposed a mathematical model to describe the superconducting phenomena from a macroscopic point of view based on the theory of secondary phase transitions proposed by Landau and named it Ginzburg-Landau theory (G-L Theory) [6-7], in which a completely new physical quantity called the G-L parameter κ was proposed to classify superconductors into two types, namely, Class I superconductors and Class II superconductors, when $\kappa < 1/\sqrt{2}$, it is a Class I superconductor, and when $\kappa > 1/\sqrt{2}$ [8-9], it is a Class II superconductor. It was not until 1957 when three scientists, J. Bardeen, L. N. Cooper and J. R. Schrieffer, proposed the BCS Theory [10] that made a historic significance to the development of superconducting materials, which also marked the gradual maturation of superconductivity theory. Although BCS Theory has some limitations and can only explain the mechanism in conventional superconducting materials perfectly, scientists did not stop at this point in the exploration of superconducting materials, and with the precipitation of time, many new superconducting materials appeared in front of human, and some of them cannot be explained by BCS Theory, such as copper-oxygen superconducting materials. Some of these superconducting materials cannot be explained by BCS theory, such as copper-oxygen superconductor materials and iron-based superconducting materials, which produce superconductivity at high temperatures. The superconductors that can be explained by BCS Theory are conventional superconductors, such as those made of alloy superconducting materials, while those that cannot be explained by BCS Theory are unconventional superconductors, such as copper-based superconductors. The superconductivity mechanism of these unconventional superconductors and the search for higher T_c superconducting materials to achieve room temperature superconductivity is one of the major challenges in the current scientific community. In addition, besides finding higher T_c superconducting materials, structural and performance characterization of superconducting materials is also a very important research direction.

3. Characterization of superconducting materials

3.1. The use of scanning tunneling microscope (STM) in the study of superconducting materials

STM is an instrument that uses a scanning probe to observe and locate an atom in a material. With its higher resolution compared to other atomic force microscopes and the ability to use the tip of the scanning probe to precisely manipulate atoms at temperatures as low as 4K, the STM is a very important tool for research at the microscopic scale. The working principle is that when a needle tip of only atomic scale size is scanned at a fixed height on the sample to be scanned, a single-electron tunneling effect in quantum mechanics is generated, and the probe will release a certain voltage in the scanned region, and a tunneling effect is generated between the probe tip and the scanned sample, allowing the escape of electrons, thus forming a tunneling current. Because the surface atoms of the sample are not horizontal, but undulating, the distance between the probe and the surface of the scanned sample is constantly changing, so the intensity of the current is a function of the distance between the probe and the scanned sample, that is, the voltage change on the surface of the sample is obtained by differentiating the

conductance and tunneling current (dI/dV), so another name for STM is scanning tunneling spectroscopy (STS). [11]

In the study of Fe-based superconducting materials, some scientists have used STM to demonstrate the hole Fermi and electron Fermi surfaces of Fe-based superconducting materials s_{\pm} . For example, Hanaguri et al. [12] performed quasiparticle interference (QPI) measurement on Fe(SeTe), a material with a magnetic field. The main conclusion is shown in Figure 1, which shows that the material Fe(SeTe) has both electron and hole Fermi surfaces, and the size of both Fermi surfaces is basically similar. The q_2 scattering between the electron-hole pockets corresponds to the scattering between the Fermi pockets with different energy band gaps, while the q_3 scattering between the electron-electron pockets corresponds to the scattering between the Fermi pockets with the same energy band gaps, considering that the energy band gaps of the electron and hole pockets are of opposite sign, i.e., s_{\pm} pairing. The measured FT-QPI image at zero magnetic field (as in Figure 1(a)) reveals that the patch of q_2 scattering between the electron-hole pockets is stronger than that of q_3 scattering between the electron-electron pockets. Starting from the two expressions of Cooper for the probability amplitude of the unoccupied and occupied $\kappa \pm$ states.

$$u_{\kappa} = \frac{\Delta_{\kappa}}{\sqrt{\Delta_{\kappa}^2 + \epsilon_{\kappa}^2}} \sqrt{\frac{1}{2} \left(1 + \frac{\epsilon_{\kappa}}{E_{\kappa}} \right)} \quad (1)$$

$$v_{\kappa} = \frac{\Delta_{\kappa}}{\sqrt{\Delta_{\kappa}^2 + \epsilon_{\kappa}^2}} \sqrt{\frac{1}{2} \left(1 - \frac{\epsilon_{\kappa}}{E_{\kappa}} \right)} \quad (2)$$

Bogoliubov coefficients u_{κ} and v_{κ} are the opposite with each other. When the sign of the energy band gap is opposite, u_{κ} and v_{κ} are the same sign of each other. In the sample material scattered with various defects and impurities can be when as non-magnetic impurities scattered in Bogoliubov quasiparticles, due to the Fermi golden rule, the intensity of scattering under the simple model is not only proportional to the initial state at scattering and the final state at scattering, but also related to the coherence factor term of the superconducting state [11].

$$I(\kappa, \kappa') = |u_{\kappa} u_{\kappa'}^* \pm v_{\kappa} v_{\kappa'}^*|^2 \quad (3)$$

Compared to the coherence factor of the same-sign scattering, the coherence factor of its opposite-sign scattering is larger, which is one of the evidences of the opposite sign of the energy band gap of the electron-hole Fermi surface. Following the previous analysis, the flux core of the material can be recognized as a magnetic scattering center after adding a magnetic field of 10T. The scattering of the order parameter anisotropic scattering is suppressed, while the isotropic scattering will be enhanced. The results of the actual measurements are in accordance with the expected results (Figure 1(d)), thus proving the opposite sign of the energy band gap between the electron and hole pockets in the Fe(SeTe) system.

Scientists generally believe that iron ions in iron-based superconducting materials are not magnetic, but atoms of elements such as cobalt and nickel doped into the lattice form ionic states, which possess properties very similar to those of the iron ion state, and their excess d electrons are added to the off-domain electrons, so they are also considered to be nonmagnetic. Experimentally, when the scattering potential of the non-magnetic impurity is very small, such as in $\text{Na}(\text{Fe}_{1-x}\text{Co}_x)\text{As}$, its Co impurity will induce the impurity state will be close to the superconducting coherent peak, but the impurity bound state cannot be observed near the zero energy [13]. Cu impurities were doped into $\text{Na}(\text{Fe}_{1-x}\text{Co}_x)\text{As}$ and magnetization measurements were used to determine whether the Cu atoms were non-magnetized or weakly magnetized impurities [14]. After using STM, the Cu atoms can be found to be doped into the position and the image of the Na atom morphology above the Cu atom is observed in Figure 2(a), and from the schematic view of the atomic distribution (Figure 2(b)), it can be judged that there is a Cu atom doped below the center of the high bright double hammer-shaped bright spot. The measurement by the scanning tunneling spectrometer shows that the Cu impurity has a great influence on the spectral shape in the energy band gap (Figure 2(c)). Subtracting the tunneling spread measured away from the impurity spot enables the difference in energy-dependent differential conductance to be obtained (as in Figure 2(d)), which can be clearly observed from the image of the impurity state within the energy band gap

induced by the non-magnetic impurity Cu atom and is in mutual agreement with the calculated results under $s \pm$ pairing, a more practical experimental evidence of the symmetry of the $s \pm$ superconducting pairing of this material [14].

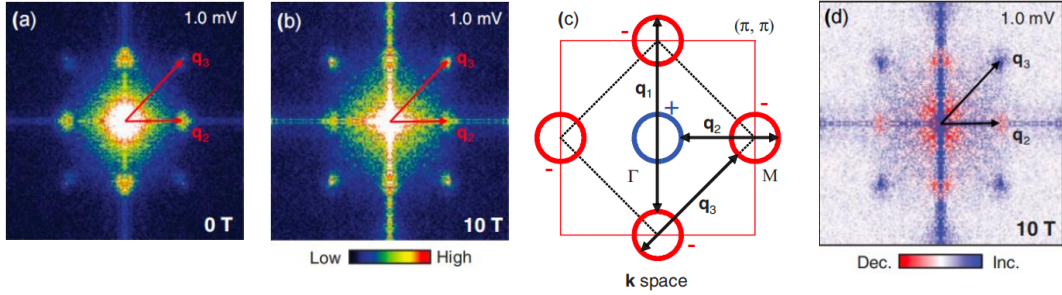


Figure 1. Variation of different scattering patch intensities in FT-QPI images of Fe(SeTe) under magnetic field. (a) and (b) FT-QPI images obtained at 10 T magnetic field intensity, respectively; (c) The Fe(SeTe) Fermi surface and the main inter-pocket scattering channel display images; (d) The result of the FT-QPI affected under magnetic field obtained by subtracting (b) figure from (a) figure, whose red color is signal weakening and blue color is signal enhancement [12].

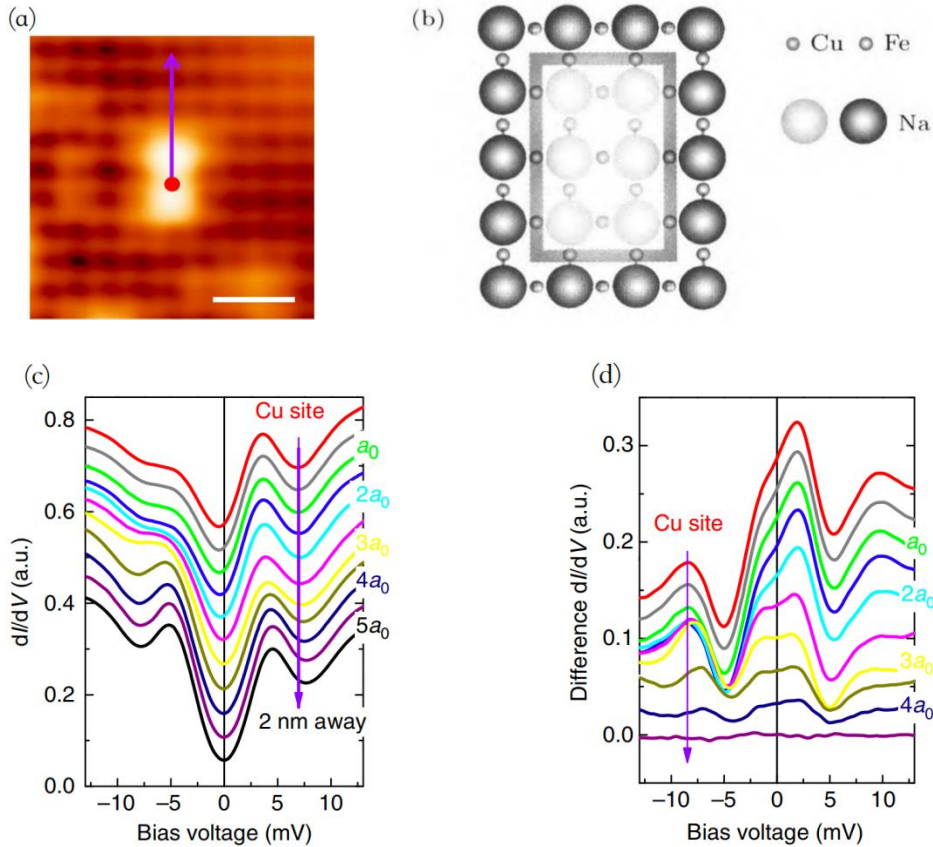


Figure 2. Non-magnetic Cu impurities induce bound states within the energy band gap. (a) Shape of Na atoms on the surface above the Cu-doped atoms measured by STM; (b) Schematic diagram of the effect of Cu atom doping on the Na atoms on the surface; (c) The tunneling spectrum measured by the arrow along (a); (d) The tunneling spectrum after subtracting 2 nm away from the impurity site and obtaining the differential conductance with spatial variation [14].

3.2. Research application of Fourier-transform infrared (FTIR) spectroscopy in superconducting materials

FTIR spectrometer is composed of Michelson interferometer and computer, where the main function of Michelson interferometer is to divide the light from the light source into two beams to form a certain degree of light range difference, and then make the two beams of light compound to produce interference. The interferometric light will meet in the beam splitter and pass through the sample cell, after which the obtained interferometric image function includes all the frequencies of the light source and its intensity information will be Fourier-transformed using a computer to obtain the material transmittance, absorbance with wave number and infrared spectra.

Infrared spectroscopy is extremely sensitive to the superconducting band gap and the possible unpaired quasiparticles within the band gap in the study of iron-based superconducting materials, so it can also be used to study the symmetry of the superconducting band gap within iron-based superconducting materials.

The superconducting material in the Ba122 system in iron-based superconducting materials is an excellent sample for experimental studies. The parent material is BaFe_2As_2 material. The parent material is doped with holes or electrons, which induces superconductivity within FeAs obtained by replacing part of the Ba atoms in the material by K atoms. Since the Ba atoms are outside the FeAs surface, this doping is usually referred to as out-of-plane doping. The electron-doped $\text{Ba}(\text{Fe}_{1-x}\text{Co}_x)_2\text{As}_2$, which is obtained by replacing part of the Fe atoms with Co atoms, is doped directly on the FeAs face, so it is usually referred to as in-plane doping. However, in-plane doping causes defects in the crystal, and these defects can be treated as non-magnetic impurities, so the FeAs face of $\text{Ba}(\text{Fe}_{1-x}\text{Co}_x)_2\text{As}_2$ has very many impurities. Comparing the spectral response of the superconducting states of the two doped materials gives important information about the symmetry of the superconducting energy band gap [15].

Figure 3 compares the photoconductivity spectra of electron-doped $\text{Ba}(\text{Fe}_{0.92}\text{Co}_{0.08})_2\text{As}_2$, at $T_c=25\text{K}$, and hole-doped $\text{Ba}_{0.6}\text{K}_{0.4}\text{Fe}_2\text{As}_2$ in the superconducting state at $T_c=38\text{K}$. The pink one is the photoconductivity curve of the hole-doped $\text{Ba}_{0.6}\text{K}_{0.4}\text{Fe}_2\text{As}_2$ becomes zero below about 160 cm^{-1} , which proves that the energy band gap is s-wave symmetric and there is no unpaired quasiparticle inside its energy band gap. In blue, the photoconductivity curve of electron-doped $\text{Ba}(\text{Fe}_{0.92}\text{Co}_{0.08})_2\text{As}_2$ shows a significant drop at low frequencies, which indicates that the superconducting band gap of the material is opened, but does not drop to zero. The low frequency photoconductivity spectrum still requires a Drude component to represent the unpaired quasiparticles, as shown in the blue shaded part, which also indicates a large number of unpaired carriers in the superconducting band gap.

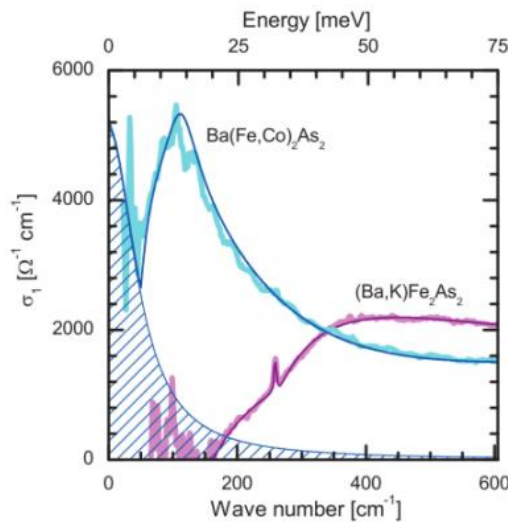


Figure 3. The photoconductivity spectra of electron-doped $\text{Ba}(\text{Fe}_{0.92}\text{Co}_{0.08})_2\text{As}_2$ and hole-doped $\text{Ba}_{0.6}\text{K}_{0.4}\text{Fe}_2\text{As}_2$ when the temperature is at 5 K [15].

The above experiments, together with the characteristics of the two samples, lead to one result. The hole-doped $\text{Ba}_{0.6}\text{K}_{0.4}\text{Fe}_2\text{As}_2$ is out-of-plane doped with a clean internal FeAs surface, and no unpaired quasiparticles are observed in the low-energy photoconductivity spectrum. The electron-doped $\text{Ba}(\text{Fe}_{0.92}\text{Co}_{0.08})_2\text{As}_2$ is in-plane doped, and a large number of nonmagnetic impurities appear in the FeAs plane of the material, which shows the Drude response for the paired alignment particles in the low-energy photoconductivity spectrum. Because of the appearance of non-magnetic impurity unpairing, it further confirms that the superconducting energy band gap symmetry in iron-based superconducting materials is s_{\pm} . The interband scattering unpairing experiments induced by nonmagnetic impurities were observed in $(\text{Li}_{1-x}\text{Fe}_x)\text{OHFe}_{1-y}\text{Zn}_y\text{Se}$ by the research group of Haihu Wen at Nanjing University in $(\text{Li}_{1-x}\text{Fe}_x)\text{OHFe}_{1-y}\text{Zn}_y\text{Se}$ using quasiparticle interference technique provides accurate evidence for the s_{\pm} symmetry of the superconducting energy band gap in superconducting materials [16].

3.3. Characterization of superconducting materials - four-probe electrical transport measurements

Solid materials all have a fundamental physical quantity: resistivity, which ranges from 10^{-8} to 10^{16} Ωcm . Metallic materials, semiconductor materials and insulator materials all have their own different resistivity magnitudes. The four-probe method is a very good choice to find out the resistivity of a material.

The principle of the four-probe electrical transport measurement method for measuring resistance is to place the current probe and the voltage probe separately, with the current probe at the ends of the measurement sample and the voltage probe in the middle of the measurement sample (Figure 4). Because the current is constant output, the current on the two current probes passing through the two ends of the measurement sample is still I . Normally the internal resistance of the voltmeter is much greater than the resistance of the measurement material itself, but according to the equivalent circuit, the current through the voltmeter is basically zero, while the current through the measurement sample is I . This also means that the potential difference generated by the two voltage probes in the middle of the measurement sample is $V = IR$, so the resistance obtained by the four-probe electrical transport measurement method is $R_{4PP} = R$. This also means that the error generated by its contact resistance on the measurement results is eliminated, and the resistance value obtained in the ideal case is the exact resistance value of its measurement sample.

As mentioned above, when performing resistance measurements on superconducting materials, the voltage signal is very small, making these tiny voltage signals very easy to be disturbed by external factors. One way is to increase the current to too high voltage signals, but the drawback is also very obvious, because when the current increases, its thermal effect will also be correspondingly strengthened, so that the temperature of the measured sample is controlled by the actual resistance. And when a low temperature environment is needed to measure superconducting materials, it is not desirable to increase the current to control the voltage error. Among the sources of voltage error is the presence of a more obvious noise, a temperature rise and fall. From the thermoelectric effect, when two materials are in contact to generate a thermocouple, and any temperature rise and fall that exists in the thermocouple will result in a potential difference between the two ends of the thermocouple, and this phenomenon is called the thermoelectric potential (V_{th}). If one wants to eliminate the thermoelectric potential, one usually uses AC measurements to counteract the generation of the thermoelectric potential, based on the principle of a DC signal V_{th} , which changes with temperature and not with current. However, if AC current is used, a new voltage error is generated, and these errors originate from the parasitic inductance and parasitic capacitance of the measurement system itself, which can generate errors at high frequencies and thus affect the final measurement results. If the DC reversal method is used for measurement, where the nature of V_{th} does not vary with current, the value obtained by subtracting the equivalent reverse current can eliminate V_{th} . In the common case, the voltage measured by the current in one direction is $V_{m1} = V_R + V_{th}$, and what is obtained after reversing the current is $V_{m2} = -V_R + V_{th} + \delta V_{th}$, and the difference between the two divided by the current can be obtained as follows:

$$R = \frac{V_{m1} - V_{m2}}{2I} = \frac{V_R + \delta V_{th}/2}{I} \quad (4)$$

And which δV_{th} is the change in the thermoelectric potential that occurs after two measurements and is proportional to the amount of change in temperature T and the amount of change in temperature is the product of the rate of change in temperature and time:

$$\Delta R = \frac{\delta V_{th}}{2I} = \frac{k\delta T}{2I} = \frac{k}{2I} \frac{d(\delta T)}{dT} \Delta t \quad (5)$$

where ΔR is the change in the thermoelectric potential produced by the resistance measurement error, k is the proportionality coefficient of the thermoelectric potential and temperature. From equation (4), it can be learned that as long as the time interval Δt between two inversion measurements is shortened and the value of its temperature change rate $\frac{d(\delta T)}{dT}$ is ensured to be small, the error can be minimized and an accurate resistance value of its measured material can be obtained [17].

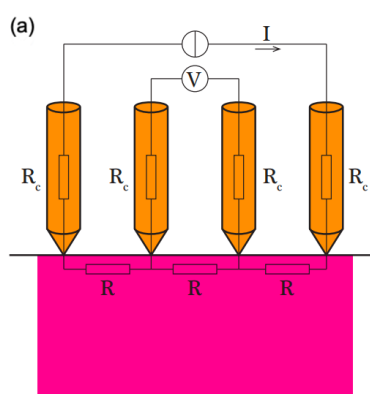


Figure 4. Four-probe electrical transport measurement method and its equivalent circuit [18].

4. The use of photoelectric effect in the study of superconducting materials

4.1. Photoelectric effect

The photoelectric phenomenon was discovered by the German physicist Heinrich Rudolf Hertz in 1887, but the correct theoretical explanation of the phenomenon was proposed by another famous physicist Albert Einstein, who won the Nobel Prize in Physics in 1921 for this theoretical achievement. It has played a significant role in the study of photons and quantum nature for future generations of scientists. It also proved the particle nature of light, with the classical examples of interference and diffraction of light. It also had a great influence on the birth of the concept of wave-particle duality.

The photoelectric effect is a very interesting and important phenomenon in physics, which mainly occurs when a beam of light with a special frequency is irradiated on the corresponding metal material. The electrons inside the metal material will absorb the energy carried by the photons injected into the material, thus forming a photocurrent, but once the frequency of the light irradiation exceeds the critical value of the metal material, also called the cut-off frequency, which is also the corresponding limit frequency of light. This critical value depends mainly on the metal material, and the energy of the emitted electrons depends on the wavelength of the light rather than the light intensity. The direction of scattering of those escaping electrons is not fixed, but mostly perpendicular to the surface of the metal material, and there is no relationship with the direction of light.

When the frequency of light exceeds the limit frequency, the surface of the metal material affected by light will immediately escape photoelectrons, thus occurring photoelectric effect. Outside the experimental metal material with a closed circuit, in addition to a positive power supply, so that all the photoelectrons will escape from the anode movement, forming a photocurrent. But the photocurrent does not become infinitely large, mainly by the number of photoelectrons limit, because the metal material can escape electrons is limited, so the phenomenon is called saturation current. In other words,

the strength of the current depends on the number of photons per unit time of incident light on the surface of the metal material, and the more photons per unit time that pass through the metal surface, the more photoelectrons will be generated, thus making the current also increase.

4.2. Application of angle-resolved photoemission spectroscopy in the study of superconducting materials

ARPES has played an excellent role in the study of the multi-orbital pair electron structure of iron-based superconducting materials, the symmetry of the superconducting energy band gap and its size, the structure of the various ordered states pair electrons and the possible electronic coupling modes that may arise.

Its working principle is based on the photoelectric effect proposed by the famous physicist Albert Einstein. When a photon is incident on a material, the electrons within the material absorb the energy of the photon and undergo an energy level jump. If the energy of the electron is greater than the work function ϕ of the material, which is usually in the range of 4 eV to 5 eV for metals, there is a certain probability that the photoelectrons will escape from the surface of the material, and the energy and momentum of the photoelectrons will be picked up by an analyzer for analysis (Figure 5). Starting from the conservation of energy and momentum in the direction parallel to the sample surface, the photoelectron energy E_{kin} and the momentum $P_{||}$ to the sample surface are obtained by two equations: $E_{kin} = h\nu - |E_B| - \phi$ and $P_{||} = \sqrt{2mE_{kin}} \cdot \sin \vartheta$. Where E_B is the electron binding energy and ϑ is the angle at which the photoelectrons are emitted. Although the momentum on the surface of the perpendicular sample is not conserved, $K_{||}$ indicates that under the constant condition. It is still possible to use the method of the internal potential to obtain the relevant information on K_{\perp} [18].

From the obtained data on electron energy as well as momentum and spin, the relationship between electron energy and momentum scattering, the distribution curves of energy and momentum of electrons, the results of Fermi and isoenergetic surfaces can be derived in order to obtain further physical quantities related to the electron velocity, effective mass, scattering and Fermi surface structure, the size of the energy band gap and its symmetry under the electronic microstructure of the material of the observed sample (see Figure 5). This technique, which can simultaneously obtain energy and momentum as well as spin-resolving capability, is not achievable by other experimental techniques, especially for the multiband properties in iron-based superconducting materials, where the role generated by the angularly resolved photoelectron energy spectrum is irreplaceable [19].

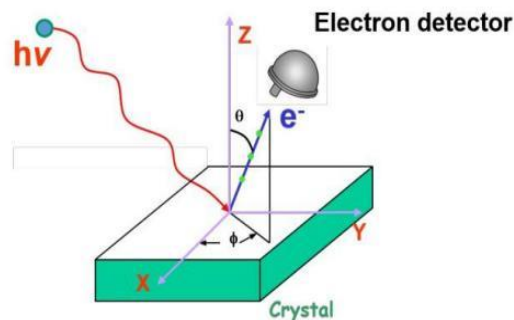


Figure 5. Schematic diagram of the principle of angle-resolved photoelectric f-energy spectrum

5. Summary and outlook

This paper mainly describes the history of superconducting materials, their morphology and various characterizations of superconducting materials, and partially summarizes the mainstream means of studying superconducting materials in the current scientific community. The future research goal for superconducting materials is inevitably to achieve room temperature superconductivity. In 2020, scientists at the University of Rochester observed that hydrogen-rich materials can achieve room-

temperature superconductivity at a temperature of about 15 degrees Celsius, or 288 K. This shows that hydrogen-rich materials are a kind of superconducting materials with great potential, so that scientists can see the hope of achieving room-temperature superconductivity, so we can boldly predict that the future realization of Therefore, we can boldly predict that hydrogen-rich materials will be used for room temperature superconductivity in the future.

References:

- [1] Li Jie, Xin Ying, Yan Guo. GBT 2900.100-2017 Electrical terminology Superconductivity: China Standards Press, 2017
- [2] Fei Youjing. Research progress and application of superconducting materials[J]. New Materials Industry,2017(7):9-12.
- [3] Duan Dinglong. Study on the temperature dependence of high-temperature superconductor resistance and Meissner effect[J]. Science and Technology Wind,2018(25):202.
- [4] London F., London H., The electromagnetic equations of the supra conductor[J]. Proceedings of the Royal Society of London Series a-Mathematical and Physical Sciences. 1935, 149 (A866): 0071-0088
- [5] Pippard. A.B., Proc. Roy. Soc., 1950, A203: 210
- [6] Sun Qingfeng. Spin superconductivity and its Ginzburg-Landau equation [C]. // Proceedings of the 12th National Conference on Magnetism Theory. 2013:33-33.
- [7] Bao, Zhiqiang. Study on the theory of spin superconductivity[D]. University of Chinese Academy of Sciences, 2015.
- [8] Zhang L. Y., Transcending freedom: magical superconductor [M]. Science Press, 2005 : 33-37
- [9] XIANG Td wave superconductor [M]. Beijing: Science Press, 2007 : 1-3
- [10] Zhao Jijun, Chen Gang. Establishment of superconducting BCS theory [J]. University Physics, 2007,26(9):46-51.
- [11] Hoffman J E 2011 Rep. Prog. Phys. 74 124513
- [12] Hanagui T, Niitaka S, Kuroki K, Takagi H 2010 Science 328 474
- [13] Yang H, Wang Z, Fang D, Li S, Kariyado T, Chen G, Ogata M, Das T, Balasky A V, Wen H H 2012 Phys. Rev. B 86 214512
- [14] Yang H, Wang Z, Fang D, Deng Q, Wang Q H, Xiang Y Y, Yang Y, Wen H H 2013 Nat. Commun. 4 2749
- [15] Dai Y M, Xu B, Shen B, Wen H H, Qiu X G, Lobo R P S M. Europhys. Lett. 2013, 104(4): 47006
- [16] Du Z, Yang X, Altenfeld D, Gu Q, Yang H, Eremin I, Hirschfeld P J, Mazin I I, Lin H, Zhu X, Wen H H. Nat. Phys. 2017, 14: 134
- [17] Ge Jianfeng. Development of STM-based microzonal four-probe and in situ measurement of interfacial superconductivity [D]. Shanghai:Shanghai Jiao Tong University,2016.
- [18] Hüfner S 1996 Photoelectron Spectroscopy (Berlin Heidelberg: Springer-Verlag
- [19] Zhao Lin, Liu Guodong, Zhou Xingjiang. Angle-resolved photoemission spectroscopy of the electronic structure of iron-based high-temperature superconductors[J]. Journal of Physics,2018,67(20):222-247.